Relay of Receptive-Field Properties in Dorsal Lateral Geniculate Nucleus of the Cat

K.-P. HOFFMANN, J. STONE, AND S. MURRAY SHERMAN

Department of Physiology, John Curtin School of Medical Research, Australian National University, Canberra, Australia 2601

THE DORSAL lateral geniculate nucleus (LGNd) of the cat is a principal relay nucleus on the direct pathway from the retina to the visual cortex, and several parameters of its organization as a relay are well established. First, relay cells of the LGNd have either on- or off-center receptive fields (16), because each relay cell receives direct excitatory drive from either on- or off-center retinal ganglion cells (6, 16). Second, retinal ganglion cells fall into two groups (X-cells and Y-cells) according to whether they sum the influences of the center and surround regions of their receptive fields linearly or nonlinearly (8). Most LGNd relay cells can be similarly classified because most receive direct excitatory drive from either X- or Y-type retinal ganglion cells (6). Third, each relay cell receives direct excitatory drive from either fast- or slow-conducting retinal afferents, and its own axon is correspondingly either fast or slow conducting (6, 36). The two latter parameters are closely correlated since Y-cells have been shown to have fast axons and X-cells, slow axons (6, 11). The on/off organization is independent of the other two parameters, however. Both Y-cells and X-cells can have either on- or off-center fields.

This report examines several features of the LGNd relay in the normal cat, extending previous concepts and establishing a spectrum of normal properties against which the properties of the LGNd in deprived cats (described in the following paper (30)), can be compared. First, the separate relay in the LGNd of the X- and Y-cell activity of the retina is described. Second, several properties of X- and Y-cells of the LGNd were observed to vary consistently with the eccentricity of their receptive fields. Specifically, variations in the relative frequency of X- and Y-cells, in their field diameter, and in the conduction velocity of their retinal afferents are described. Third, evidence is presented that the inhibitory mechanisms of the LGNd are less specifically organized than the direct excitatory relay.

Received for publication December 27, 1971.

METHODS

General preparation

Experiments were performed on 20 adult cats. They were anesthetized with ether for the initial surgical preparation. During recording the cats were anesthetized with nitrous oxide (70% N_2O, 30% O_2) and kept paralyzed by a continuous intravenous infusion of gallamine triethiodide (Flaxedil, 16.2 mg/hr) and toxiferine dichloride (Hoffman-LaRoche, 1 mg/hr) in saline (6.5 ml/hr). Details of the stereotaxic apparatus and standard head position used are available in earlier papers (19, 21).

Physiological recording

Units were recorded in the LGNd with 4 M NaCl-filled micropipettes of resistance 6–15 megohms (measured at 50 Hz). The LGNd was approached stereotaxically. Layer A of the LGNd was usually located 12–14 mm from the cortical surface. To distinguish postsynaptic spike responses from antidromic and presynaptic orthodromic responses we relied on previously established criteria (2, 23). The two most useful were the variability in spike latency to a suprathreshold stimulus (always greater in postsynaptic responses) and the ability of presynaptic responses to follow high-frequency (>150 Hz) stimulation.

Electrical stimulation

Electrical stimuli were 50- to 100-μ sec pulses from a Tektronix 161 pulse generator, delivered

through a Bioelectric Instruments ISB isolation unit. With the stimulating electrodes used (Rhodes Medical Instruments type NE-100), the amplitude of the stimulus pulses was approximately linearly related to the amplitude setting on the pulse generator, with a maximum of 15 v. Amplitude values given in the text are the voltages applied to the electrodes.

A pair of stimulating electrodes was placed stereotaxically in the optic chiasm (OX position). The target coordinates of the tips were anterior 15 mm, right lateral and left lateral 2 mm, and depth 20–23 mm below the surface of the cortex. The final depth of the OX electrodes was fixed while recording in the LGNd, with a low-resistance (<5 megohms) micropipette, the field potential elicited by OX stimulation. At depths greater than 20 mm below the cortical surface the threshold electrical stimulus for eliciting the presynaptic components of the LGNd field response always fell sharply. Dissection following several initial experiments showed that a threshold of about 1.75 v for a 50-μ sec pulse was obtained when the stimulating electrode tips just contacted the dorsal surface of the chiasm and that the threshold dropped further when the electrodes penetrated the chiasm. In subsequent experiments the OX electrodes were fixed when the stimulus threshold reached 1.75 v. For activating LGNd units antidromically, wire electrodes (1-mm bare tips) were inserted 1–2 mm into the visual cortex (VC position). The area of cortex used was bounded by the stereotaxic coordinates anterior 0 to −5 mm, lateral 0 to 5 mm. This is the area of cortex to which the area centralis and the surrounding 5–10° of visual field project (19). It is mainly area 17 but includes part of the 17–18 border (ref 19).

Visual stimulation

Atropine was used to dilate the cats' pupils, and Neo-Synephrine to retract their lids and nictitating membranes. Zero-power contact lenses and 3-mm-diameter artificial pupils were used. In addition, spectacle lenses were commonly needed to achieve optimal focus of the eyes on the tangent screen and these lenses were mounted just in front of the artificial pupils. The appropriate spectacle lens power was determined by testing the responses of a unit to a series of hand-moved gratings of decreasing spatial frequency (6).

The visual stimuli were stationary spots of light, hand-held black targets, and hand-held black and white, square-wave gratings. The luminance of the spots of light was approximately 140 cd/m^2. The luminances of the black targets and the black bars in the gratings were approximately equal at 5–10 cd/m^2. The luminances of the tangent screen and of the white bars of the grating were approximately equal at 70 cd/m^2. This luminance is high in the mesopic range of the cat (7). Stimulus timing was monitored by a light-dependent resistor. The resistor has an aperture of 2.5 mm which was held 2–3 mm away from the surface of the tangent screen, at a location appropriate for it to monitor luminance changes generated by the stimuli (see Fig. 1).

Measurement of receptive-field size and eccentricity

We measured the size of only the center region of each receptive field. The great majority of these centers were plotted on a frontal tangent screen, 1 m from the nodal points of the cat's eyes, with small (0.1–1.0°) flashing spots of light. The remaining centers (from cells in the left LGNd) were located more than about 55° to the cat's right and were plotted on a parasagittal tangent screen located 1.5 m from the nodal point of the cat's right eye. To plot each of the smallest center regions, which were only slightly bigger than the smallest test spot, we first located the position of the center region. We then sequentially moved the test spot, flashing at about 2 Hz, toward the center region from positions above, below, to the left of, and to the right of the center until a weak center response was first elicited. The spot was held at this position and the edge of the spot closest to the receptive-field center was marked. This procedure was repeated several times to ensure accurate location of the four marks. The perimeter of the receptive-field center was assumed to be approximately circular or elliptical and to pass through the four marks. Larger receptive fields were also plotted by moving a small flashing spot within the center region (cf. Rodieck and Stone, ref 25). When applied to the same receptive field the two methods yielded essentially identical results. We measured the width of each field center along the axis of the field perpendicular to the line joining the field to the projected position of the area centralis (see below) and calculated the angular subtense of this width at the nodal point of the eye.

Receptive-field eccentricity was measured with respect to the position of the projection of the area centralis. This position was estimated as follows. The blind spots were projected onto the tangent screen using the technique described by Fernald and Chase (9). We assumed from previous work (22, 39) that on a 1-m tangent screen the projection of the area centralis is located 28 cm medial to and 13 cm

below the center of the blind spot. In several experiments we were also able to locate the zero meridian of the visual field of each eye by the technique of Sanderson and Sherman (29), and this passed within 1.5 cm of the previously determined location of the projection of the area centralis.

Terminology

Several terms used throughout this paper are defined below.

Y-cell (following Enroth-Cugell and Robson, ref 8) is used to refer to either a retinal ganglion cell or an LGNd cell with Y-type properties. A Y-afferent is the axon of a retinal Y-cell. A Y-field is the receptive field of a Y-cell. X-cell, X-afferent, and X-field are used analogously.

The binocular segment of the LGNd is defined, following Guillery and Stelzner (13), as the medial, laminated segment of the nucleus, in which adjacent laminae receive afferents from opposite eyes. The monocular segment of the LGNd is the smaller, lateral, unlaminated crescent which receives input from only the contralateral eye. The binocular and monocular segments of the visual field can then be defined as those portions of visual field represented in, respectively, the binocular and monocular segments of the LGNd. The maps of Sanderson (27) provide an estimate of the lateral extent of the binocular segment of the visual field.

RESULTS

Single-unit recording

The present study concerns principally the properties of 284 LGNd cells but three other types of units were also observed. First, 40 optic tract fibers were identified by the location at which they were recorded (i.e., in the deeper layers of and deep to the LGNd), by their brief, positive-going action potentials and by their presynaptic response to OX stimulation (see METHODS). Second, 34 optic radiation units were distinguished from LGNd cells by their waveform and by the location at which they were recorded (above the LGNd). Data taken from radiation units have been excluded, except from the account of inhibitory mechanisms in the LGNd. Third, we occasionally encountered units which responded to both OX and VC stimulation with a late (5–6 msec latency) postsynaptic burst of spikes. None of this third group had the clear-cut on- or off-center receptive fields typical of LGNd cells (16). Several did have more-or-less definable receptive fields, giving on-off responses to flashing-spot stimuli. They were most commonly recorded at locations just dorsal to the LGNd (cf. Sanderson, ref 27). Some of their properties suggest that they are interneurons (cf. Burke and Sefton, ref 4, 5) and they are not considered further here.

Of the 284 LGNd cells, 85 were positively identified as relay cells, being activated both orthodromically by OX stimulation and antidromically by VC stimulation. Many cells could not be activated antidromically, presumably because their axons did not pass sufficiently close to a VC electrode. In addition, VC electrodes were not used either in the experiments in which we sought populations of units with highly eccentric fields, because of the difficulty of access to the areas of cortex involved, or in the experiments which were principally concerned with inhibitory influences in the LGNd. The other 199 LGNd cells had OX latencies and receptive-field properties essentially identical with those of the 85 identified relay cells and we assume here that all 284 were relay cells.

The X/Y properties of all cells were tested. The OX latencies of 275 were measured (97%). The receptive-field centers of 240 units (85%) were accurately plotted. The remaining units were lost before an accurate field plot was completed.

Receptive-field classification

Except for a small minority (discussed further below), all LGNd and optic radiation units could be classified as X-cells or Y-cells. The optic tract units tested could all be similarly classified. In making the classification we relied on three tests, described by previous authors (6, 11, 26).

First, X-cells generally respond in a "tonic" (11, 26) or "sustained" (6) manner when a stimulus spot of the appropriate contrast (and somewhat smaller than the receptive-field center) is introduced into the field center. Thus when a light spot flashes on in the center of an on-center field (Fig. 1*A*) or a black spot is brought quickly into the center of an off-center field (Fig. 1*C*) the cell's firing rate is increased and is maintained at a rate higher than the spontaneous level until the spot is removed.

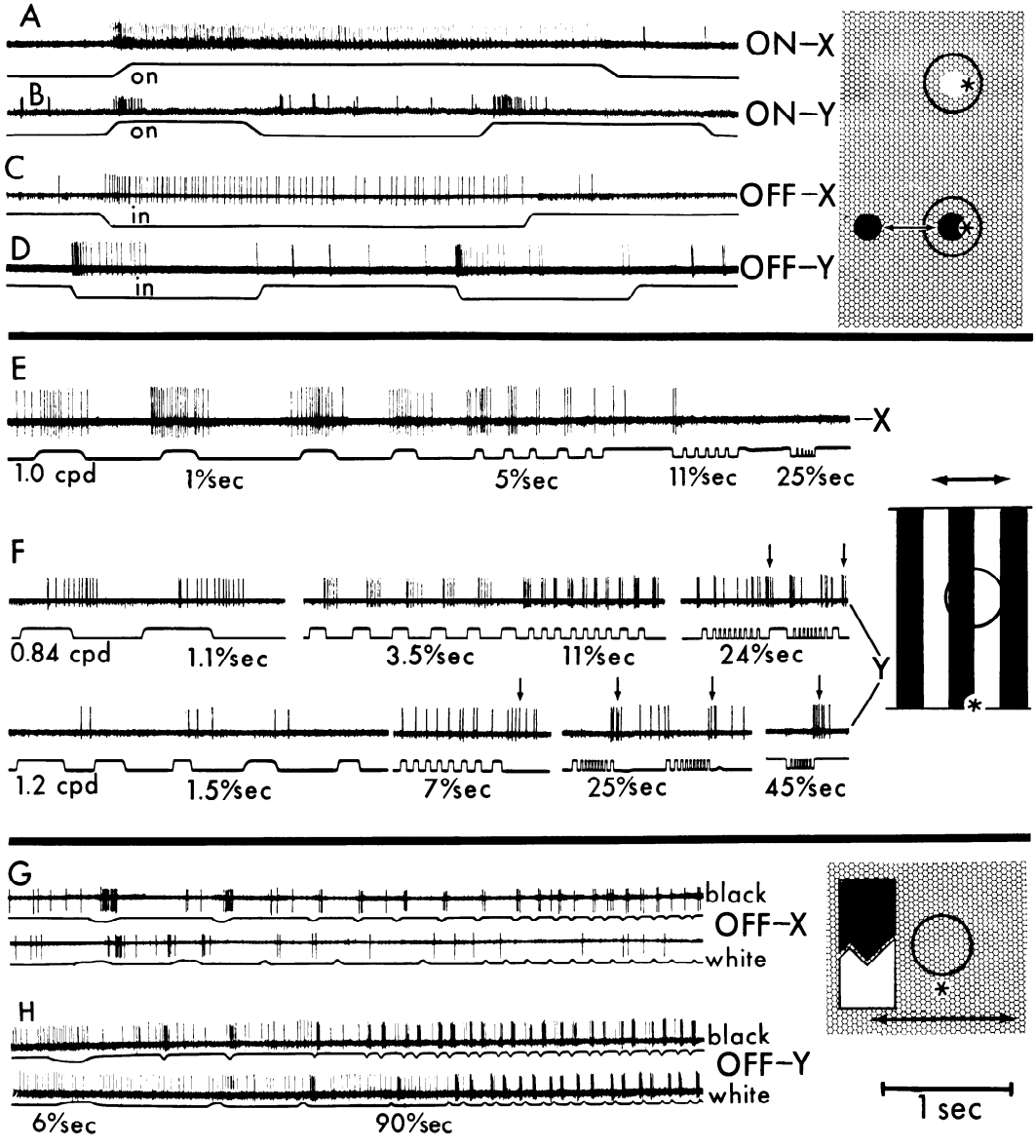

FIG. 1. Characteristic responses of X- and Y-cells to visual stimuli. Below each spike trace is a trace showing changes in luminance in the region of the receptive field monitored by a light-sensing device (whose position is indicated with an asterisk in diagrams on the right-hand side of the figure). In each case the luminance trace goes up as the monitored luminance increases, down as it decreases. *A–D*: responses to stationary stimuli. *A*: on-center X-cell responds to a centered spot of light with a burst of firing which is maintained above spontaneous level as long as the spot is on. *B*: on-center Y-cell responds to same stimulus with only a transient burst of spikes. A typical stimulus situation is shown at right. The spot is centered within the center region of the receptive field. *C*: response of an off-center X-cell to a black target moved into the field center and held stationary is maintained as long as the target is present. *D*: response of an off-center Y-cell to the same stimulus is a transient burst of spikes. Typical stimulus situation is shown at right. *E–F*: responses of X- and Y-cells to grating stimuli. *E*: an X-cell responds to each cycle of a slowly moving (1°/sec) 1 cycle/degree grating, but fails to respond at high speeds (25°/sec). This cell had an off-center field, 0.6° in diameter. *F:* upper spike trace shows a Y-cell responding to each cycle of a slowly moving (1°/sec) 0.84 cycle/degree grating. At higher speeds of movement (24°/sec) it fails, like an X-cell, to respond to each cycle of the grating, but gives a single-burst response (marked by arrows). The cell responded only weakly (lower spike trace) to a slow movement of a somewhat finer grating (1.2 cpd), but gave strong burst responses (arrowed) to higher speeds of movement. This cell had an off-center field, 1.1° in diameter. A typical stimulus situation is shown at right. *G–H:* differences in speed selectivity of X- and Y-cells. *G:* upper spike trace shows that an off-center X-cell responds to slow and fast movements of a black bar swept across its receptive field. The lower spike trace shows that the cell responds only to slower movements of a white bar. For this test the black and white bars were moved across a gray background of luminance 35 cd/m². *H:* a Y-cell (off-center in this case) responds well to slow and fast movements of stimuli of either contrast. A typical stimulus situation is shown at right. The 1-sec scale applies to all of *A–H*.

By contrast, Y-cells respond to the same stimuli with only a "phasic" (11, 26) or "transient" (6) burst of spikes (Fig. 1*B* and *D*).

Second (this test follows Cleland et al., ref 6), X-cells respond to moving gratings in only one manner, which is by firing to each cycle of the grating. Figure 1*E* shows an X-cell firing strongly to each cycle of a slowly moving (1°/sec) grating whose spatial frequency was 1 cycle/degree (1 cpd). The cell responds progressively less strongly to movements at 5°/sec and 11°/sec, and is entirely unresponsive at 25°/sec. As the spatial frequency of the stimulus grating is increased the responses of an X-cell are progressively restricted to slower speeds of movement, and above a certain spatial frequency the cell is entirely unresponsive to any speed. The upper response trace in Fig. 1*F* shows that a Y-cell also responds vigorously to each cycle of a coarse (0.84 cpd) grating moved slowly. As in an X-cell the response to each cycle weakens as stimulus speed is increased, and at above 24°/sec this cycle-locked response fails. A qualitatively different response is then elicited from a Y-cell. This is a single burst of firing to a fast movement of the grating during which several cycles of the grating cross the receptive field. Response bursts of this type are indicated by arrows in Fig. 1*F*, upper and lower response traces. Y-cells typically respond in this way to gratings finer than the finest to which they respond in a cycle-locked manner. The lower response trace in Fig. 1*F*, for example, shows that this Y-cell responded only weakly to slow movements of 1.2 cpd grating, but responded with vigorous single bursts (arrowed) to fast movements.

Third (cf. Cleland et al., ref 6), X-cells fail to respond to fast movements of targets larger than their field centers, especially when the contrast of the target is appropriate for inhibiting the center (e.g., a large white spot crossing an off-center field as in Fig. 1*G*). By contrast a Y-cell responds clearly to fast movements of large targets of either contrast (Fig. 1*H*).

No one of these tests was perfectly reliable. From about 10% of units, for example, the stationary spot elicited a response which, despite careful focusing of the eye and centering of the spot, was not clearly sustained or transient, and in such cases the other tests were relied on. Only five cells could not be clearly classified as predominantly X- or Y-type, and these have been excluded from Figs. 3, 4, and 5.

Latency relationships

Responses of five LGNd cells to OX stimulation are shown in Fig. 2. In each the action spike is seen superimposed on a field potential. Features of the spike discharge have been described in an earlier report (36). Two of these features need emphasis here. First, for each unit there is some variation in the latency of the spike, a variation typical of a postsynaptic discharge (2, 23). Second, the latency range in any unit is much less than the latency range of the population of units. This suggests that each cell receives its excitatory drive from one afferent or from a number of afferents with very similar conduction velocities (6, 36).

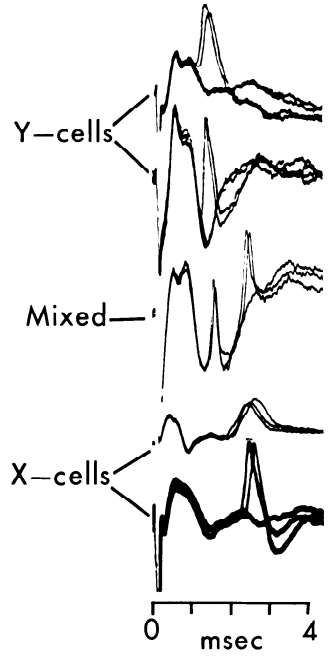

FIG. 2. Sample traces of the spike responses of LGNd cells to OX stimulation. In each the spike is superimposed on the LGNd field potential. The upper two traces show Y-cells, the lower two traces show X-cells. The middle trace shows an unusual cell (only two observed) which responded with two spikes. The early spike has a latency typical of a Y-cell, the latter spike of an X-cell.

OX latency was measured for each unit from the beginning of the stimulus artifact to the middle of the latency range of the foot of the action spike. Figure 3*A* shows the frequency/latency histogram for the LGNd cells studied. Y-cells respond at shorter latencies than X-cells, with some overlap. The histogram is, in fact, bimodal, the first peak consisting entirely of Y-cells, and the second predominantly of X-cells.

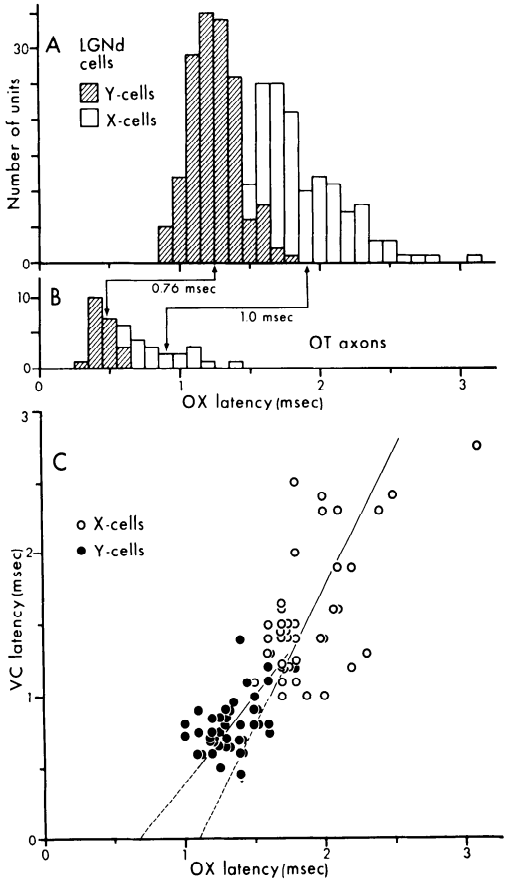

FIG. 3. *A:* frequency histogram showing the OX latencies obtained for 275 of the 284 cells studied. *B:* frequency histogram showing the OX latencies of 40 optic tract (OT) axons recorded just deep to the LGNd. Y-afferents are represented by the hatched segments, X-afferents by the open segments. The difference in mean OX latency between OT axons and LGNd cells is shown separately for Ys (0.76 msec) and Xs (1.0 msec). *C:* graph showing the relation between the OX latency and VC latency of 85 LGNd relay cells. Y-cells are plotted with closed circles, X-cells with open circles. The orthogonal regression lines for the X- and Y-cells are drawn separately, and their extrapolations to the abscissa are shown.

This latency difference between the cell types is apparent in the illustrated responses of Y-cells (Fig. 2, upper two traces) and X-cells (Fig. 2, lower two traces). A comparable latency difference was seen for optic tract fibers (Fig. 3*B*). Two LGNd cells responded to OX stimulation with two spikes; an example is illustrated in Fig. 2, middle trace. The early spike has a latency (1.2 msec) typical for a Y-cell, and the later spike has a latency (2.4 msec) typical for an X-cell. These two units were among the five which had mixed X- and Y-properties, and are not included in Fig. 3*A*. This evidence of direct convergence of X- and Y-afferents on a small minority of LGNd cells confirms a previous report (6).

Two inferences can be drawn from these results. The first concerns synaptic discharge delay in X- and Y-cells. In a preliminary report (36) evidence was presented of a delay of 0.6 msec in a fast-responding LGNd cell between the invasion of the afferent terminals and the onset of the postsynaptic discharge. Figure 3*A* and *B* shows that the mean OX latency of Y-afferents was 0.76 msec shorter than the mean OX latency of Y-cells in the LGNd. For X-afferents and X-cells the difference was 1.0 msec. These latency differences include time for invasion of the afferent terminals as well as for synaptic discharge delay so that these figures indicate that synaptic discharge delay is less than 0.8 msec for Y-cells, and less than 1.0 msec for X-cells. Terminal invasion is presumably slightly quicker in Y-afferents, so that synaptic discharge delay may be essentially identical for X- and Y-cells, approximately 0.6–0.8 msec.

The second inference concerns the conduction velocities of X- and Y-afferents. The most common Y-cell latency to OX stimulation was 1.2–1.3 msec. Assuming 0.75 msec for synaptic discharge delay and 20 mm for the conduction distance from optic chiasm to the axon terminals in the LGNd (35), the predominant afferent conduction velocity for Y-cells was 36–44 m/sec. Estimated in the same way, the predominant afferent velocity for X-cells was 19–24 m/sec. Similar velocity values are obtained from the latencies of Y- and X-type optic tract fibers (Fig. 3*B*). These two velocity groupings correspond closely to the two pre-

dominant conduction velocity groups of the optic nerve described by earlier workers (1, 3, 35, 38). Longer latency X-cells suggest the presence of considerable numbers of slower-conducting fibers, corresponding (36) to the slower conduction velocity groups described by Stone and Freeman (35, and see below).

The antidromic responses of LGNd cells to VC stimulation are described in a previous report (36). Figure 3*C* shows the correlation between the OX and VC latencies and the X/Y classification of 85 units. The correlation between OX and VC latencies is statistically significant for the total population ($r = 0.84$, $P < 0.001$) and for the X-cells ($r = 0.62$, $P < 0.001$) and Y-cells ($r = 0.48$, $P < 0.001$) considered separately. LGNd cells driven by fast afferents have fast axons projecting to visual cortex and Y-fields. Cells innervated by slow afferents have slow axons and X-fields. The orthogonal regression lines for Y-cells and X-cells are shown. Their abscissa intercepts are 0.67 msec for the Y-cells and 1.1 msec for the X-cells. Thus, if afferent conduction time (OX latency less the delay of transmission in the LGNd estimated from Fig. 3*A* and *B*) were plotted against antidromic conduction time for each unit, both lines would run close to the origin. Thus, for Y- and X-cells, mean antidromic conduction time is proportional to mean afferent conduction time, without an additive constant. The slopes of the regression lines are 1.2 for the Y-cells and 1.9 for the X-cells, and the difference in slope is statistically significant ($P < 0.001$ in a test for parallel regression lines (42)). The afferent conduction distance (about 20 mm (35)) is similar to the antidromic distance (15–20 mm (2, 40)), so that the greater-than-unity slopes of the regression lines suggest that, on the average, retinal afferents to a LGNd cell are faster conducting than its axon and that this conduction velocity difference is more marked for X-cells.

Eccentricity relationships

The sample of 284 LGNd cells was divided into five groups according to the eccentricity of their receptive fields from the area centralis. Three groups cover the eccentricity ranges 0–3, 3–10, and 10–20°. The fourth group (20° – M) includes all receptive fields with eccentricities greater than 20°, but located within the binocular segment of the visual field (see METHODS). The fifth group (M) includes all receptive fields located in the monocular segment of the visual field. These limits were chosen to provide direct comparison with the following paper (30). For fields not far above or below the zero horizontal of the visual field (this includes a majority of the present sample) the latter two groups cover the eccentricity ranges 20° to about 45°, and greater than about 45°, respectively.

Figure 4*A* shows the variation with eccentricity in the mean OX latency of X- and Y-cells. Mean latency is plotted with open circles for X-cells and with closed circles for Y-cells. The vertical bars indicate the ranges of OX latencies about each mean. The mean latency of X-cells in the most central (0–3°) group is significantly greater than in the adjacent (3–10°) group ($P < 0.01$ on a t test), but there is no significant change between adjacent peripheral groups. The same trend is apparent, though less marked, among the Y-cells. Figure 4*B* shows that in our data the relative frequency of Y-cells (expressed as a percentage of the total of X- and Y-cells) increases with eccentricity. The percentage of Y-cells increases sharply from 34% in the 0–3° group to 51% in the adjacent group, and continues to increase with eccentricity to 73% in the most peripheral group. The statistical significance of this trend was established in two ways. First, the points deviate significantly from a horizontal line through the mean percentage (55%) of Y-cells ($P < 0.005$ on a χ^2 test). Second, for 59 electrode tracks we noted the value of the term $Y - X$ (number of Y-cells minus number of X-cells), and the mean eccentricity of the receptive fields. $Y - X$ was significantly and positively correlated with mean eccentricity ($r = 0.36$, $P < 0.01$). Figure 4*C* shows the variation with eccentricity in the mean diameter of X-field centers (open circles), of Y-field centers (closed circles), and of all fields (triangles). Within each eccentricity group the mean diameter of Y-fields is always greater than of X-fields ($P < 0.01$ on a t test for each group). For both X- and Y-cells mean size increases with

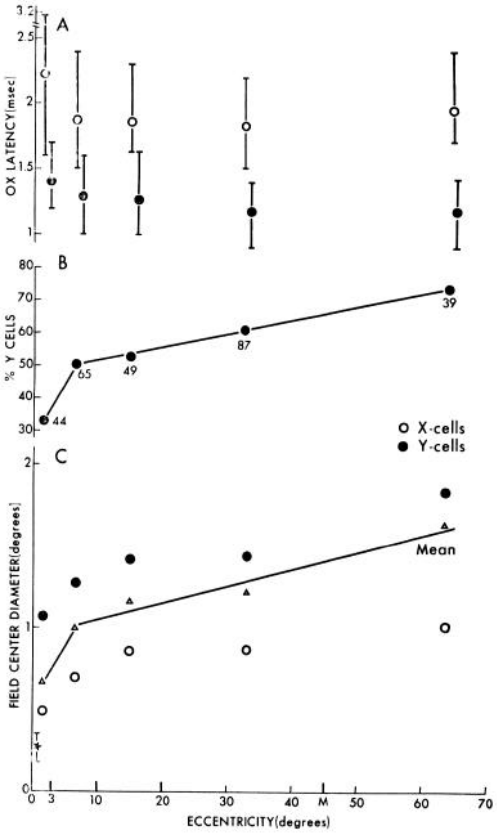

FIG. 4. For this figure the LGNd cells were divided into five eccentricity groups (see text). *A:* for each eccentricity group the mean OX latency of Y-cells (closed circles) and of X-cells (open circles) is plotted, and for each mean the vertical bars represent the range of observed values. *B:* the percentage of Y-cells (number of Y-cells as a percentage of the total of X- and Y-cells) is plotted for each eccentricity group. The number of cells in each eccentricity group is shown. *C:* for each eccentricity group the mean diameter of the center regions of the receptive fields is plotted with a closed circle for Y-cells, and with an open circle for X-cells. The mean diameter of all fields in a group is plotted with a △ symbol. The ★ symbol represents the mean center diameter of 12 X-fields which were recorded along two electrode tracks, and which were the smallest in the 0–3° eccentricity group. The vertical bar represents the range of their field center diameters about this mean. Ranges of field center diameters observed in all eccentricity groups are shown in Fig. 5.

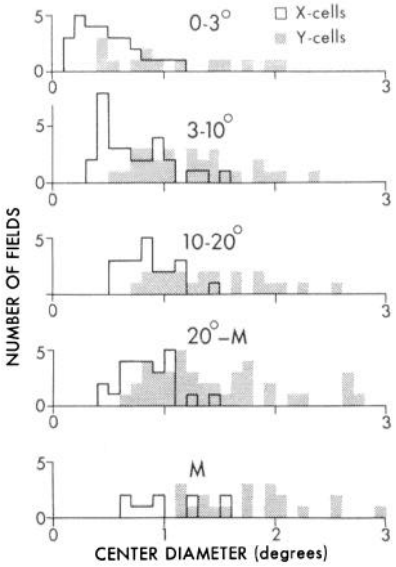

FIG. 5. Frequency histograms of receptive-field center diameters. The 240 receptive fields were divided into five eccentricity groups (cf. Fig. 4 and see text) and a separate histogram is drawn for the X- and Y-cells in each group.

eccentricity, particularly between 0 and 20°. The mean diameter of all fields increases more markedly than does the mean diameter of X- or Y-fields alone, because of the accompanying increase in the relative frequency of Y-cells (Fig. 4*B*). Figure 5 shows the frequency distribution of field center sizes in each eccentricity group. In all groups, there is a considerable overlap in the ranges of X- and Y-field diameters.

Three possible sources of error in the data presented in Figs. 4 and 5 need consideration. First, there is a residual error of about ±2° in locating the projection of the area centralis by the methods used (22), an error quite large relative to the extent of the central (0–3°) eccentricity group. It seems likely that this group includes cells which should be in the adjacent (3–10°) group and vice versa. Certainly, the smallest fields observed (<0.35° in diameter) were grouped along two electrode tracks, and all fell in the 0–3° group. Their mean field center size is plotted with a star symbol in Fig. 4*C*; the vertical bar represents the range of their field sizes. All had OX latencies longer than 2 msec. Thus, more dramatic changes in field size and OX latency between the two central eccentricity groups might be obtained if the error in locating the area centralis could be reduced. Second, it is possible that different electrodes, because of variations in their tip size, configuration, or electrical resistance, tended to pick up X- and Y-cells in dif-

ferent ratios. Third, it is possible that X- and Y-cells are not randomly mixed in the LGNd, but are grouped together. The latter two factors would both tend to increase the variability in the relative frequency of X- and Y-cells recorded on individual tracks and to increase the frequency with which long sequences of one type of cell were recorded. There was, in fact, considerable variability between electrode tracks, in the relative frequency of X- and Y-cells recorded, and sequences of as many as six X- or Y-cells were commonly found. However, a number of statistical tests showed that neither the variability in relative numbers of X- and Y-cells nor the observed sequences of X- and Y-cells differed significantly from what would be expected if the electrodes had identical sampling properties and were sampling a random mixture of X- and Y-cells. Because of the large variations between electrode tracks, the cells in each eccentricity group in Fig. 4 were pooled from at least four to eight electrode tracks, each having more than six units, and taken from at least three experiments.

Convergence of X- and Y-inhibition

The evidence (presented above and elsewhere (6)) that X and Y afferents do not converge on LGNd relay cells, refers only to the principal excitatory action of these afferents. The initial excitatory effect of an afferent volley to the LGNd is followed by prolonged inhibition. In both the rat (4, 5) and cat (20, 32) the inhibitory mechanism involves interneurons, intrinsic to the LGNd, which are activated by collaterals of relay cell axons and inhibit relay cells. In the cat the interneurons may also be directly excited by retinal afferents (20). The following evidence suggests that the inhibitory mechanisms elicited in the LGNd by X- and Y-afferents do converge onto LGNd relay cells.

In a series of three experiments the threshold OX stimulus for every LGNd and optic radiation unit encountered was measured as follows. We used a stimulus pulse of constant 50-μsec width and variable amplitude, and for each unit counted the number of times (N) it discharged during sequences of 10 stimuli delivered at 1 Hz. Some cells, particularly Y cells, had very clear thresholds. N increased from 0 to 10 over a small voltage range and threshold was taken as the middle of this range. For the Y-cell in Fig. 6*E*, for example, N increased from 0 to 10 over a voltage change from 0.2 to 1.1 v, and threshold was taken as 0.65 v. Threshold was less clear in many cells in which N did not reach 10 at any stimulus strength. Threshold was then taken as the middle of the voltage range over which N increased from 0 to its maximum value. This is illustrated for an X-cell in Fig. 6*E*. The threshold of this cell was taken as 8.5 v.

Figure 6*B–D* shows three histograms. Each is a frequency/threshold histogram for the units tested in a different experiment. In each experiment the threshold for Y-cells was consistently lower than for X-cells. The same differential threshold is demonstrated in Fig. 6A. These traces show the field potential generated at the optic disc by OX stimulation. The potential has two major components, fast and slow. These are generated, respectively, by the fast-conducting axon group (3) (which comprises Y-afferents (6, 11, and see above)) and by the slow-conducting axon group (which comprises X-afferents (6, 11, and see above)). The Y-afferents have the lower threshold. Moreover, at stimulus levels above 2.55× threshold the fast potential does not increase in amplitude (i.e., all fast fibers are being discharged), but the slower potential is still submaximal. Thus stimulus increments above 2.55× threshold bring in only high-threshold slow fibers.

Figure 6*F* and *G* show recovery-of-responsiveness curves for two LGNd cells and present the evidence that both X- and Y-cells show signs of inhibitory influences generated by both classes of afferents. In each case the cell's responsiveness following an OX stimulus was estimated from its response to the second of two OX stimuli. The intensity of the second (test) shock was fixed at a threshold or just suprathreshold value. The intensity of the first (conditioning) shock was varied in fixed steps, as was the interval between shocks. For each intensity level of the conditioning shock and for each step in the interstimulus interval, we counted the number of times (N) the unit responded during a series of 10 test

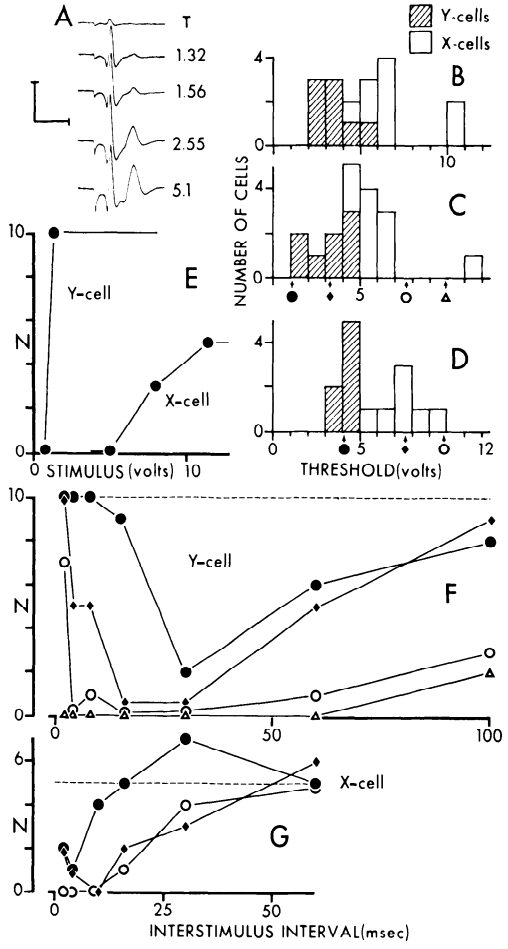

FIG. 6. Results of experiments demonstrating the convergence of inhibitory influences in the LGNd. *A:* field potentials elicited by OX stimulus and recorded at the optic nerve head. Stimulus amplitude was threshold (T) for the top trace. Numbers at the right of the lower traces give stimulus amplitude as a multiple of T. Two components can be distinguished (35). The early (fast conducting, Y-afferent) component has the lower threshold (top trace) and reaches its maximum to a 2.55× threshold stimulus. The later (slow conducting, X-afferent) component has a higher threshold (second trace) and increases in amplitude after the early component has reached its maximum. The scale lines represent 4 mv and 2 msec. *B–D:* frequency-threshold histograms for all the LGNd units tested in three different experiments. In each the Y-cells have the lower threshold to OX stimulation. Arrows and symbols in *C* and *D* indicate, respectively, the conditioning stimulus levels used for the Y-cell tested in *F* and for the X-cell tested in *G*. *E:* graph of N (number of times the cell discharged to a sequence of 10 OX stimuli) as a function of stimulus amplitude for the Y-cell tested in *F* and for the X-cell tested in *G*. *F:* two-shock test of a Y-cell: graph of N for the test stimulus as a function of the interstimulus interval. Four strengths of conditioning stimulation were used and changes in N following each conditioning level are plotted with different symbols. The actual conditioning levels are indicated in *C*, with the appropriate symbol. Thus, symbols ●, ◆, ○ and △ indicate increasing strengths of the conditioning stimulus. The horizontal broken line represents the value of N for the unconditioned test stimulus. *G:* two-shock test of an X-cell. Three levels of conditioning stimulation were used (●, ◆, △) as indicated in *D*. The horizontal broken line represents the value of N for the unconditioned test stimulus.

shocks. The unit of Fig. 6*F* was a Y-cell. The conditioning stimulus was first set at 1 v, a voltage which excited (Fig. 6*C*) only the lowest threshold Y-cells. This stimulus produced a marked depression of N with an onset latency of 16 msec. With a conditioning stimulus of 3.2 v, which should still excite only Y-cells (Fig. 6*C*), the depression of N was greater and began at shorter (8 msec) latency. When the conditioning stimulus was increased to 7.5 v, causing the discharge of X-cells as well as Y-cells, N was depressed sooner, more completely, and for a longer period. A further increment in the conditioning stimulus to 10 v caused the discharge of an increasing proportion of X-cells (Fig. 6*C*) and caused a further increase in the depression of N. A comparable series of recovery curves obtained for an X-cell are shown in Fig. 6*G*.

There are a number of qualifications to this result which must be stated. First, the time course of the recovery of responsiveness varied considerably between cells, although no consistent difference was apparent between Y- and X-cells. Second, in some cells inhibition of firing was apparent only if the test shock was close to threshold, and in other cells no inhibition of firing could be detected. Third, some cells responded too unreliably to OX stimulation to be tested. Nevertheless, inhibition of the type illustrated in Fig. 6*F* and *G* was clearly demonstrable in 15 of the 21 units tested, and these qualifications do not seem to affect our basic point: this is that the responsiveness of both Y- and X-cells is suppressed (i.e., the cells are inhibited) by stimuli which are weak enough to excite only Y-cells, and further, the strength of this suppression increases as the strength of the conditioning stimulus is increased over

a range which brings in only high-threshold X-cells. Thus both X- and Y-cells seem to receive inhibitory influences elicited in the LGNd by both X- and Y-afferents.

DISCUSSION

X–Y terminology

In their original report, Enroth-Cugell and Robson (8) chose the noncommittal terms X and Y to refer to the linear and nonlinear types of cat retinal ganglion cell. Saito et al. (26) and Fukada (11) chose similarly noncommittal terms (type II and type I). On the other hand, Cleland et al. (6) chose terms (sustained and transient) which are descriptive of one of the characteristic differences between the two types. The descriptive terms have definite advantages, but the sustained-transient distinction is only one of a range of distinguishing properties and it is not yet established, for example, which of these properties are important in subsequent cortical processing. Some discussion of this problem is presented below, but until more is known of the functional significance of X/Y differences there may be some advantage in using noncommittal terms.

Implications of LGNd relay of X- and Y-afferents

Perhaps the most striking feature of the relay in the LGNd of X- and Y-afferents is that there is markedly little convergence of the two afferent types in their direct excitatory action on LGNd relay cells. As a consequence most LGNd cells have either X-properties or Y-properties and relay them separately to the visual cortex. Hoffmann and Stone (14) have recently presented evidence, based on latency measurements to electrical stimulation, that many complex cells of the visual cortex (first described by Hubel and Wiesel, ref 17) receive strong, direct (i.e., monosynaptic), excitatory input from the fast-conducting radiation axons. Conversely, simple cells (17) and possibly also hypercomplex cells (18) seem to receive direct excitatory input from the slower radiation axons. In the present context the inference can be drawn that complex cells receive afferents from Y-cells of the LGNd and simple cells from X-cells. It is interesting, therefore, to note similarities between the receptive-field properties of these different cells. The excitatory zones of complex fields are larger than those of simple fields (14, 17, 24) and, correspondingly, the center regions of Y-fields are larger than those of X-fields (6, 8, 11, and Fig. 5). Simple fields are markedly more selective for slow speeds of stimulus movement than are complex fields (14, 24) and, correspondingly, selectivity for slow speeds is apparent in X-cells and not in Y-cells (Fig. 1*G*, *H*, and ref 6).

The above evidence that complex and simple cells receive a qualitatively different input from the LGNd adds weight to a previous suggestion (14) that the two types may be processing visual afferent information in parallel. However, it should be stressed that X–Y differences do not determine all the differences between cortical cells. For example, a sustained-transient distinction has not been described for cortical cells. Some of the responses of simple cells to flashing spot stimuli described by Hubel and Wiesel (15) would be classified as sustained (Fig. 1 in ref 15) and others as transient (Fig. 2 in ref 15). Flashing spot stimuli are ineffective for many complex cells and evoke on-off responses in others (17). Conversely, prominent features of cortical cells, such as orientation- and direction-selectivity, are not at all apparent in X- and Y-cells and the transformation of receptive-field properties between the LGNd and visual cortex seems much greater than between retina and LGNd (17). The two properties which distinguish X- and Y-cells and which appear also to distinguish their probable target cortical cells are, by present account, speed selectivity and receptive-field size.

Eccentricity relationships

There is a statistically significant decrease in the mean OX latency of X-cells between the 0–3° eccentricity group and the adjacent (3–10°) group, but no significant difference between any other two adjacent groups (Fig. 4*A*). A similar, though less marked, trend is apparent among the Y-cells. Thus there appears to be little change with eccentricity in the afferent latency of either X- or Y-cells, except in the immediate

vicinity of the area centralis. This confirms an earlier analysis of the variation of conduction velocity with retinal eccentricity (35). The longer latency of both X- and Y-cells at the area centralis is in good agreement with the conduction velocity groupings suggested by Stone and Freeman (35), and with Stone and Holländer's (37) observation that the axons arising from the area centralis ganglion cells are smaller than peripheral axons, and with Guillery's (12) observation that, following enucleation of one eye, the degenerating axons which reach the area centralis portion of the LGNd are finer than the axons reaching the remainder of the nucleus.

The increase in the relative frequency of Y-cells with eccentricity (Fig. 4*B*) is statistically significant, and the same trend is apparent in Fukada's (11) sample of retinal receptive fields. It is also supported by the amplitude of the fast- and slow-conducting components of the antidromic field potentials recorded in the retina by Stone and Freeman (35). At the area centralis the slow-conducting component (which is presumably generated by axons of X-cells) is predominant. Conversely, the fast-conducting component (presumably generated by Y-cell axons) is the more prominent at locations outside the area centralis. Nevertheless, there is probably need for caution in accepting Fig. 4*B* as an accurate description of the relative frequency of Y-cells. It is likely that Y-cells are larger than X-cells, for they have faster axons (see above) and larger receptive fields. It is possible that, as a result of their larger size, Y-cells were preferentially isolated by our electrodes. This caveat does not seem, however, to invalidate the general trend of results in Fig. 4*B*. Before leaving this point it should perhaps be emphasized that the increase with eccentricity in the relative frequency of Y-cells does not imply an increase in their absolute frequency. It is likely that in the LGNd (28) as in the retina (33) the total number of cells involved in the representation of unit area of the visual field decreases with eccentricity. The increase with eccentricity in the relative frequency of Y-cells probably results largely from a marked concurrent decrease in the absolute frequency of X-cells.

The larger size of Y-fields (Fig. 5) is in agreement with previous reports (6, 8, 11), as is the increase with eccentricity in the mean diameter of all receptive fields (10, 16, 28, 34, 41). One clear inference from the present results is that a major component of the increase in mean diameter is the accompanying increase in the relative frequency of Y-cells.

Organization of inhibitory mechanisms of LGNd

There seems to be a striking difference between the excitatory and inhibitory mechanisms of the LGNd in the specificity of their organization. The excitatory relay is organized so that there is little or no convergence onto individual cells of afferents from on- and off-center retinal cells (6, 16), or of axons from X- and Y-cells of the retina (see above and ref 6), or of fast- and slow-conducting axons (6, 36). The present results (Fig. 6) indicate that inhibitory influences elicited by X- and Y-afferents are not restricted to any subgroup of LGNd cells, i.e., they converge onto both X- and Y-cells. While Singer and Creutzfeldt (31) argued that the inhibitory mechanisms of the LGNd are organized with respect to the on/off classification ("reciprocal lateral inhibition") their more recent work (32) has suggested that the inhibitory influences elicited in the LGNd by on- and off-center retinal ganglion cells converge onto both on- and off-center LGNd cells. In general, the inhibitory mechanisms of the LGNd seem to be much less specifically organized than the direct, excitatory relay, and it seems possible that all LGNd relay cells receive their inhibition from the same pool of interneurons.

SUMMARY

1. The responses of 284 relay cells in the cat's dorsal lateral geniculate nucleus (LGNd) were studied. Each was classified as an X-cell or a Y-cell by its responses to visual stimuli. The latency of the orthodromic discharge of each cell following electrical stimulation of the optic chiasm (OX) was measured. For each of 85 cells, the latency of its antidromic discharge following electrical stimulation of the visual cortex was also measured.

2. Y-cells receive fast-conducting afferents from Y-type retinal ganglion cells, and have fast axons projecting to the visual cortex. Conversely, X-cells receive slow-conducting afferents, from X-type retinal ganglion cells, and have slow-conducting axons projecting to the visual cortex. Evidence of direct convergence of X- and Y-afferents onto the same LGNd relay cells was seen in only 2 of the 284 cells studied.

3. Y-cells were a minority of the cells with receptive fields located at the area centralis. The percentage of Y-cells increased steadily with receptive-field eccentricity, reaching 73% at the far periphery.

4. At all eccentricities the receptive-field centers of Y-cells are, on the average, larger than the field centers of X-cells. For both X- and Y-cells, field center size increases with eccentricity. Because of the concurrent increase in the relative frequency of Y-cells, the mean size of all fields increases more markedly than does the mean size of either X-fields or Y-fields alone.

5. In contrast to the specific organization of the direct excitatory action of X- and Y-afferents, the inhibitory influences elicited in the LGNd by X- and Y-afferents appear to converge onto single LGNd cells.

ACKNOWLEDGMENTS

We thank Miss Sandra Watson for her technical help and Mrs. Lyn Speight for her secretarial assistance. Professor P. O. Bishop gave valuable advice in the preparation of the manuscript.

S. M. Sherman was supported by National Institutes of Health Grant 1 FO2 NS4 3310.

K.-P. Hoffmann was partially supported by a travel grant from the Deutsche Forschungsgemeinschaft.

Present address of K.-P. Hoffmann: Max Planck-Institut für Psychiatrie, 8000 Munich 40, Kraepelinstr. 2, West Germany.

Present address of S. M. Sherman: Dept. of Anatomy, School of Medicine, University of Pennsylvania, Philadelphia, Pa. 19104.

REFERENCES

1. Bishop, G. H. and Clare, M. H. Organization and distribution of fibers in the optic tract of the cat. *J. Comp. Neurol.* 103: 269–304, 1955.
2. Bishop, P. O., Burke, W., and Davis, R. Single unit recording from antidromically activated optic radiation neurons. *J. Physiol., London* 162: 432–450, 1962.
3. Bishop, P. O., Jeremy, D., and Lance, J. W. The optic nerve. Properties of a central tract. *J. Physiol., London* 121: 149–152, 1953.
4. Burke, W. and Sefton, A. J. Discharge patterns of principal cells and interneurones in lateral geniculate nucleus of rat. *J. Physiol., London* 187: 201–212, 1966.
5. Burke, W. and Sefton, A. J. Inhibitory mechanisms in lateral geniculate nucleus of rat. *J. Physiol., London* 187: 231–246, 1966.
6. Cleland, B. G., Dubin, M. W., and Levick, W. R. Sustained and transient neurones in the cat's retina and lateral geniculate nucleus. *J. Physiol., London* 217: 473–496, 1971.
7. Daw, N. W. and Pearlman, A. L. Cat colour vision: one cone process or several? *J. Physiol., London* 201: 745–764, 1969.
8. Enroth-Cugell, C. and Robson, J. G. The contrast sensitivity of retinal ganglion cells of the cat. *J. Physiol., London* 187: 517-552, 1966.
9. Fernald, R. and Chase, R. An improved method for plotting retinal landmarks and focusing the eyes. *Vision Res.* 11: 95–96, 1971.
10. Fischer, B. and May, H. U. Invarianzen in der Katzenretina: Gesetzmässige Beziehungen zwischen Empfindlichkeit, Grösse and Lage receptiver Felder von Ganglienzellen. *Exptl. Brain Res.* 11: 448–464, 1970.
11. Fukada, Y. Receptive field organization of cat optic nerve fibers with special reference to conduction velocity. *Vision Res.* 11: 209–226, 1971.
12. Guillery, R. W. The laminar distribution of retinal fibers in the dorsal lateral geniculate nucleus of the cat: a new interpretation. *J. Comp. Neurol.* 138: 339–368, 1970.
13. Guillery, R. W. and Stelzner, D. The differential effects of unilateral lid closure on the monocular and binocular segments of the dorsal lateral geniculate nucleus in the cat. *J. Comp. Neurol.* 139: 413–422, 1970.
14. Hoffmann, K.-P. and Stone, J. Conduction velocity of afferents to cat visual cortex: a correlation with cortical receptive field properties. *Brain Res.* 32: 460–466, 1971.
15. Hubel, D. H. and Wiesel, T. N. Receptive fields of single neurones in the cat's striate cortex. *J. Physiol., London* 148: 574–591, 1959.
16. Hubel, D. H. and Wiesel, T. N. Integrative action in the cat's lateral geniculate body. *J. Physiol., London* 155: 385–398, 1961.
17. Hubel, D. H. and Wiesel, T. N. Receptive fields, binocular interaction and functional architecture in the cat's visual cortex. *J. Physiol., London* 160: 106–154, 1962.
18. Hubel, D. H. and Wiesel, T. N. Receptive fields and functional architecture in two nonstriate visual areas (18 and 19) of the cat. *J. Neurophysiol.* 28: 229–289, 1965.
19. Joshua, D. E. and Bishop, P. O. Binocular single vision and depth discrimination. Receptive field disparities for central and peripheral vision and binocular interaction on peripheral

single units in cat striate cortex. *Exptl. Brain Res.* 10: 389–416, 1970.

20. KATO, H., YAMAMOTO, M., AND NAKAHAMA, H. Intracellular recordings from the lateral geniculate neurons of cats. *Japan. J. Physiol.* 21: 307–323, 1971.
21. KINSTON, W. J., VADAS, M. A., AND BISHOP, P. O. Multiple projections of the visual field to the medial portion of the dorsal lateral geniculate nucleus and the adjacent nuclei of the thalamus of the cat. *J. Comp. Neurol.* 136: 295–316, 1969.
22. NIKARA, T., BISHOP, P. O., AND PETTIGREW, J. D. Analysis of retinal correspondence by studying receptive fields of single units in cat striate cortex. *Exptl. Brain Res.* 6: 353–372, 1968.
23. NODA, H. AND IWAMA, K. Unitary analysis of retinogeniculate response times in rats. *Vision Res.* 7: 205–213, 1967.
24. PETTIGREW, J. D., NIKARA, T., AND BISHOP, P. O. Responses to moving slits by single units in cat striate cortex. *Exptl. Brain Res.* 6: 373–390, 1968.
25. RODIECK, R. W. AND STONE, J. Analysis of receptive fields of cat retinal ganglion cells. *J. Neurophysiol.* 28: 833–849, 1965.
26. SAITO, H., SHIMAHARA, T., AND FUKADA, Y. Four types of responses to light and dark spot stimuli in the cat optic nerve. *Tohoku J. Exptl. Med.* 102: 127–133, 1970.
27. SANDERSON, K. J. The projection of the visual field to lateral geniculate and medial interlaminar nuclei in the cat. *J. Comp. Neurol.* 143: 101–118, 1971.
28. SANDERSON, K. J. Visual field projection columns and magnification factors in the lateral geniculate nucleus of the cat. *Exptl. Brain Res.* 13: 159–177, 1971.
29. SANDERSON, K. J. AND SHERMAN, S. M. Nasotemporal overlap in visual field projected to lateral geniculate nucleus in the cat. *J. Neurophysiol.* 34: 453–466, 1971.
30. SHERMAN, S. M. HOFFMAN, K.-P., AND STONE, J. Loss of a specific cell type from dorsal lateral geniculate nucleus in visually deprived cats. *J. Neurophysiol.* 35: 532–541, 1972.
31. SINGER, W. AND CREUTZFELDT, O. Reciprocal lateral inhibition of on and off-centre neurones in the lateral geniculate nucleus in the cat. *Exptl. Brain Res.* 10: 311–330, 1970.
32. SINGER, W., PÖPPEL, E., AND CREUTZFELDT, O. Inhibitory interaction in the cat's lateral geniculate nucleus. *Exptl. Brain Res.* 14: 210–226, 1972.
33. STONE, J. A quantitative analysis of the distribution of ganglion cells in the cat's retina. *J. Comp. Neurol.* 124: 337–352, 1965.
34. STONE, J. AND FABIAN, M. Specialized receptive fields of the cat's retina. *Science* 152: 1277–1279, 1966.
35. STONE, J. AND FREEMAN, R. B. Conduction velocity groups in the cat's optic nerve classified according to their retinal origin. *Exptl. Brain Res.* 13: 489–497, 1971.
36. STONE, J. AND HOFFMAN, K.-P. Conduction velocity as a parameter in the organisation of the afferent relay in the cat's lateral geniculate nucleus. *Brain Res.* 32: 454–459, 1971.
37. STONE, J. AND HOLLÄNDER, H. Optic nerve axon diameters measured in the cat's retina: some functional considerations. *Exptl. Brain Res.* 13: 498–503, 1971.
38. SUMITOMO, I., IDE, K., IWAMA, K., AND ARIKUNI, T. Conduction velocity of optic nerve fibers innervating lateral geniculate body and superior colliculus in the rat. *Exptl. Neurol.* 25: 378–392, 1969.
39. VAKKUR, G. J., BISHOP, P. O., AND KOZAK, W. Visual optics in the cat, including posterior nodal distance and retinal landmarks. *Vision Res.* 3: 289–314, 1963.
40. VASTOLA, E. F. Conduction velocities in single fibers of the visual radiation. *Exptl. Neurol.* 7: 1–12, 1963.
41. WIESEL, T. N. Receptive fields of ganglion cells in the cat's retina. *J. Physiol., London* 153: 583–594, 1960.
42. *Wissenschaftliche Tabellen: Documenta Geigy* (7th ed.). Basel, Switzerland: Geigy, 1969, p. 179.